CANOPUS – A GROUND-BASED INSTRUMENT ARRAY FOR REMOTE SENSING THE HIGH LATITUDE IONOSPHERE DURING THE ISTP/GGS PROGRAM

G. ROSTOKER and J. C. SAMSON
Canadian Network for Space Research and Department of Physics, University of Alberta, Edmonton, Alberta, Canada T6G 2J1

F. CREUTZBERG, T. J. HUGHES, D. R. McDIARMID, A. G. McNAMARA, A. VALLANCE JONES and D. D. WALLIS
Herzberg Institute of Astrophysics, National Research Council of Canada, Ottawa, Ontario, Canada K1A 0R6

and

L. L. COGGER
Canadian Network for Space Research and Department of Physics and Astronomy, University of Calgary, Calgary, Alberta, Canada T2N 1N4

(Received 9 March, 1993)

Abstract. Proper interpretation of *in situ* satellite data requires a knowledge of the global state of the magnetosphere-ionosphere system. CANOPUS is a large-scale array of remote sensing equipment monitoring the high latitude ionosphere from the north–central to the north–west portion of North America. The array comprises thirteen magnetometers and riometers, four meridian scanning photometers, a digital allsky imager and an auroral radar linked by geostationary satellite to a central receiving node in Ottawa, where the data are archived and made available in near real time to participating scientists. This paper provides a technical description of the various instruments in the CANOPUS array, and contains a summary of the key parameters which will be provided to the Central Data Handling Facility (CDHF) located at NASA/Goddard Space Flight Center, for use by the ISTP/GGS community.

1. Introduction

In the early days of space science, most observations of the space environment involved remote sensing from the Earth. Considering that the closest researchers could get to the space plasma environment and to the electric currents that couple the magnetosphere to the ionosphere was $\sim$ 100 km, it was striking how much information could be obtained. Long before rockets and satellites were launched allowing *in situ* measurements to be made, the existence and structure of the ionosphere had been established. The presence of electric currents was established from ground based measurements and the component currents of the substorm had been identified (viz., the directly driven currents by Vestine and Chapman (1938) and the substorm current wedge by Birkeland (1908)). Even the presence of the plasmapause had been identified using whistler measurements (cf., Carpenter, 1963). With the launches of satellites in the modern era, it would have seemed that there was no longer a need for ground based measurements. While it was true

Space Science Reviews **71:** 743–760, 1995.

that satellites revealed the particle and field configuration of the magnetosphere in a way that no ground based experiments could do, it has turned out that all that was learned was the average configuration of the magnetosphere. It has become painfully apparent that a single point of data in space and time is quite unable to permit one to define the physics of the processes which regulate the solar- terrestrial interaction and magnetosphere-ionosphere coupling.

While most space researchers recognize the need for ground based data in the study of transient variations in the solar terrestrial interaction, many workers still continue to describe the global state of the magnetosphere by either appealing to an index (e.g., AE, K_p, D_{st}) or to a single magnetogram (and often only the north–south component of the perturbation field). To those specializing in ground based remote sensing, it is quite clear that only an appropriate array of ground based instrumentation is capable of effectively defining the background state and dynamic variations of the magnetosphere-ionosphere system. Fledgling attempts to use arrays were very successful in the past in examining the dynamics of substorms as reflected in the changes of the auroral oval. Jelly and Brice (1967) used a north-south array of riometers to define the poleward motion of the disturbed oval during substorm activity. Kisabeth and Rostoker (1974) were able to use a meridian line of magnetometers to track the stepwise poleward development of the substorm westward electrojet during expansive phase activity, and Wiens and Rostoker (1975) used an east-west line of magnetometers to show that this stepwise motion was mirrored in the azimuthal expansion of the disturbed region to the west.

The rationale for ground-based measurements as a powerful tool in the hands of the space researcher has been put forward earlier by Rostoker (1990). For the purpose of this paper, we shall concentrate on the most important capability – namely, that of permitting the researcher to acquire an instantaneous picture of the two-dimensional distribution of ionospheric currents, plasma flow, particle precipitation and auroral luminosity over a significant portion of the polar ionosphere. The importance of this can be seen as one considers that any region of the magnetosphere maps to the ionosphere along magnetic field lines. That is, the ionosphere represents one boundary of the volume of space in which magnetosphere-ionosphere coupling takes place and a proper array of ground-based remote sensing equipment can provide the boundary conditions at any instant of time which are relevant to the volume of space in which spacecraft may be making sparse measurements. Over the past two decades, different groups have developed modeling techniques which permit the key electromagnetic parameters of the ionosphere to be established using physically meaningful equations and certain assumptions about ionospheric properties which are not readily measurable, specifically ionospheric conductivity (cf., Mishin *et al.*, 1980; Kamide *et al.*, 1981; Feldstein *et al.*, 1984; Richmond and Kamide, 1988). Thus, ground-based magnetic and electric field data can go a long way toward establishing the instantaneous cross-polar cap potential drop and the distribution of field-aligned currents threading the auroral oval.

While many scientists use magnetometer data to diagnose the level of magnetospheric activity, very few have the opportunity to use optical data to follow the evolution of the auroral activity. This is because the instruments that are capable of acquiring data that can be analysed quantitatively (viz., digital imagers and multi-wavelength scanning photometers) have, in the past, been operated primarily in an expeditionary fashion with the data remaining in the hands of the experimenter. While the use of optical data is limited to periods of darkness for conditions when the sky is free of clouds, information on the auroral luminosity can assist in accurately (viz., to within a few kilometers) identifying the locale of specific auroral activations and in providing an estimate of regions of the ionosphere which feature enhanced conductivity. It is worth noting that magnetometers are unable to yield information about the location of ionospheric currents to an accuracy of anything better than the Earth-ionosphere separation (viz., 100 km). In terms of assessing the magnitude of the ionospheric conductivity, information regarding the hardness of the precipitating electron spectrum is extremely valuable (cf., Rees, 1989). Scanning photometers that monitor key auroral wavelengths can provide such information, which provides a useful constraint for evaluating the Hall and Pedersen conductivities used in quantitative assessments of the character of magnetosphere-ionosphere coupling. Thus, for detailed studies of the characteristics of spatially localized events (such as substorm expansive phase development) optical data provide information of critical importance if one is to be able to use appropriate conductivity distributions for input into modeling routines such as those alluded to in the paragraph above.

For the reasons cited above, the Canadian space science community decided in the late 1970's to devote considerable resources to developing a ground based array of instrumentation which could, for specific events, provide information on the ionospheric electric fields, currents and conductivity that could be used to quantitatively assess an area of the auroral ionosphere over a spatial dimension which was sufficiently large to permit the study of the structure of regions of disturbance associated with such important phenomena as substorms . They recognized that the data should be available in near real time in order to be able to use it as a guide for initiating expeditionary research activities. (Preliminary efforts in this direction have been made at the University of Alaska, as described by Akasofu *et al.* (1992).) They further recognized that the data ought to be made available in an easily accessible data base. Since late 1989, the CANOPUS array that was developed to achieve these ends has been fully operational. In the next section of this paper we introduce the instrumentation, and we will conclude the paper by discussing some of the science that can be achieved in the context of examples of the data which will be available to the solar-terrestrial physics community as part of the ISTP/GGS mission.

2. The CANOPUS Array

The development of the CANOPUS array began in the early 1980's as a consequence of an agreement between NASA and the National Research Council of Canada designed to permit Canadian researchers to participate in the OPEN (Origin of Plasmas in the Earth's Neighbourhood) Program. Instrument development in the CANOPUS program proceeded slowly as there was a considerable amount of innovation required to construct state-of-the-art detectors and the complex data handling system. Some components of the system came on line within five years of the start of the Program, notably the auroral radar BARS. It was not until December 1989 that the full CANOPUS network became operative, and excellent data have been obtained since that time. The components of CANOPUS and their acronyms are as follows:

ASI	Allsky Imager
BARS	Bistatic Auroral Radar
MARIA	Magnetometer and Riometer Array
MPA	Meridian Photometer Array

The data collection system (DCS) and the data analysis network (DAN) form the backbone of the system through which data from the various instruments are made available.

Figure 1 shows the locations of the various sites belonging to the CANOPUS array, and Table I gives the coordinates and the complement of instrumentation located at each of those sites. It can be seen that the core of the array involves a north-south line of magnetometers and riometers passing through the well-known auroral oval site of Fort Churchill, and an east–west array stretching along the average latitude of the auroral oval from the Churchill line westward to the border between Canada and the state of Alaska. The sites of Contwoyto Lake, Fort Smith and Fort McMurray constitute a short north–south line approximately one time zone west of the Churchill line. By using data from the U.S. station of Newport, WA (NP) and Meanook, AB (MN) to the south and Cambridge Bay, NWT (CB) and Resolute Bay, NWT (RE) to the north, one has the ability to put together excellent coverage along the Alberta line using the data in a retrospective fashion.

Meridian scanning photometers strategically located along the Churchill line give virtually complete coverage of the auroral luminosity along the meridian through Fort Churchill at the key wavelengths associated with typical auroral luminosity. The north–south line of three photometers is complemented by a fourth unit located at Fort Smith, giving some indication of the gross azimuthal continuity of the auroral oval over approximately one time zone. The digital allsky imager located at Gillam, at the intersection between the Churchill and east–west lines, provides a quantitative measure of auroral luminosity at key wavelengths over the observing area shown in Figure 1. A portion of the area of the high latitude ionosphere monitored by the allsky imager is the site of the converging beams of

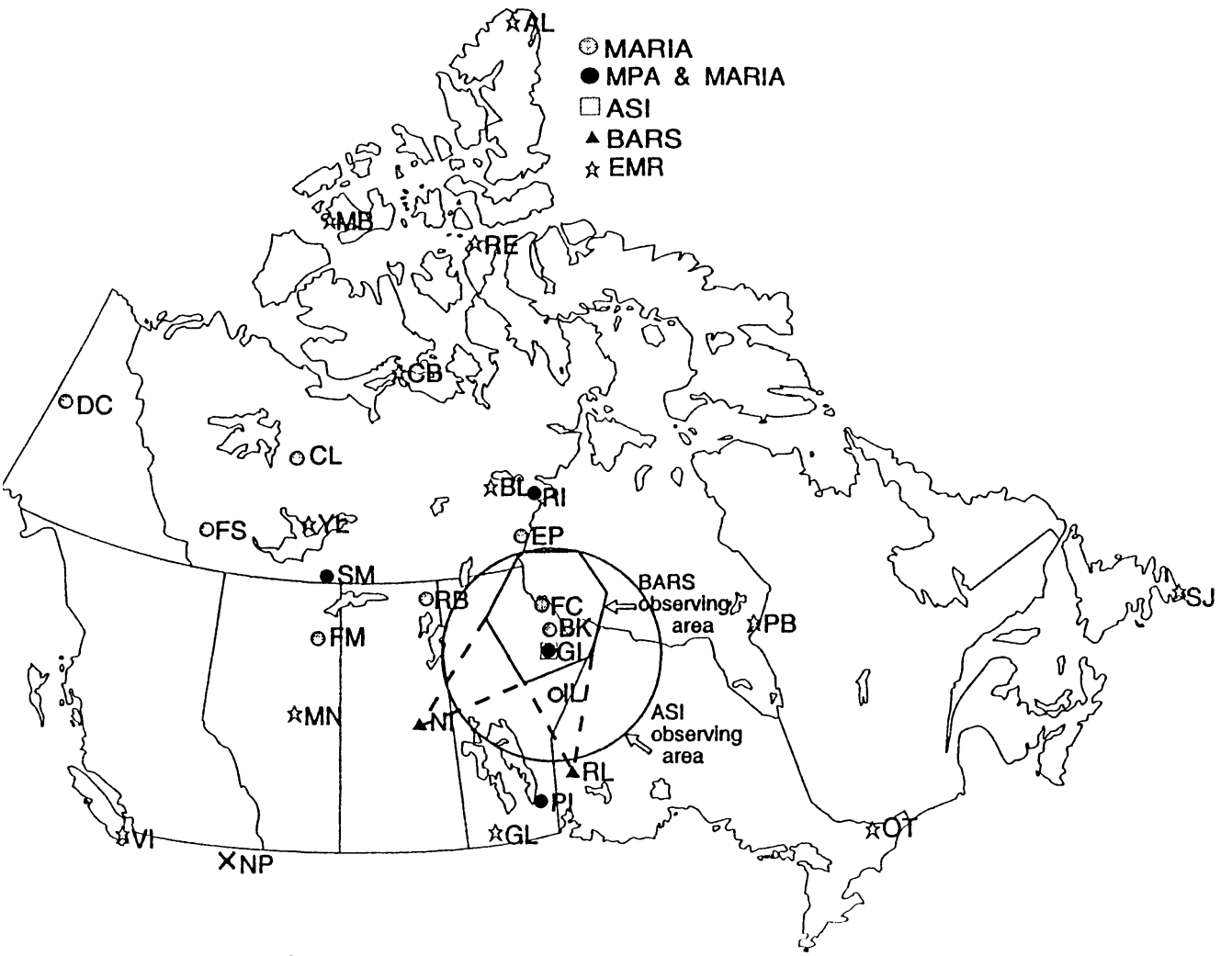

Fig. 1. Location of the CANOPUS stations and a summary of the instrumentation at each site. Also shown are the locations of magnetometers operated by the Geological Survey of Canada of Department of Energy Mines and Resources Canada (EMR). Magnetometer data from the EMR array can be obtained to supplement CANOPUS data for retrospective studies, and some of the EMR data can be accessed rapidly through the Intermagnet program.

the auroral radar which, under active conditions, is able to provide a measure of the auroral electric field over the region shown in Figure 1. In its entirety, the array is a powerful tool for diagnosing the spatial and temporal variations in the auroras and in the geomagnetic field over a large portion of the North American continent. In the next section we shall outline the technical details of each of the instruments operative in the CANOPUS array.

3. The CANOPUS Instrumentation

3.1. ALLSKY IMAGER (ASI)

This instrument operates as an allsky camera with a field of view of 160 deg using, as a detector, a single stage microchannel intensifier fiber, optically coupled to a

TABLE I

CANOPUS instrument sites

Location	Station Acronym	Geographic		Pace[b]		L	Instr.[a]
		Lat.	Long.	Lat.	Long.		
Back	BK	57.7	265.8	68.72	−30.58	7.5	M
Contwoyto LK	CL	65.8	248.8	73.43	−61.23	12.4	M
Dawson	DC	64.1	220.9	65.93	−90.08	5.9	M
Eskimo Point	EP	61.1	266.0	71.93	−31.75	10.2	M
Ft Churchill	FC	58.8	265.9	69.72	−30.76	8.2	M
Ft McMurray	FM	56.7	248.8	64.81	−54.37	5.5	M
Ft Simpson	FS	61.7	238.8	67.62	−69.86	6.8	M
Ft Smith	SM	60.0	248.1	67.92	−57.29	7.1	M P
Gillam	GI	56.4	265.4	67.38	−30.93	6.7	M P I
Island Lake	IL	53.9	265.3	64.94	−30.33	5.5	M
Nipawin	NI	53.5	256.3	63.20	−43.10	4.9	R
Pinawa	PI	50.2	264.0	61.16	−31.58	4.3	M P
Rabbit Lake	RB	58.2	256.3	67.77	−45.04	6.9	M
Rankin Inlet	RI	62.8	267.9	73.72	−28.97	12.4	M P
Red Lake	RL	50.9	266.5	62.20	−28.00	4.5	R

[a] M = Magnetometer, riometer, tellurics (MARIA).
P = Meridian photometer (MPA).
I = All-sky imager (ASI).

[b] See Baker and Wing (1989) for a description of eccentric PACE invariant coordinates.

charged- coupled device (CCD) imaging array. The pixel array is 256 × 256 with the pixel size being 44μ × 44μ (reduced to 22μ × 22μ on the CCD array by a 2:1 fiber optic taper). The photocathode of the sensor is an S20/S25 extended red type and the optics are $f/1.2$ telecentric.

Images can be obtained with an exposure time of as little as 104 ms although, during normal operation, a typical exposure time is 1.7 s. Different wavelengths are sampled using a filter wheel that features four two-inch interference filters each with a nominal 20 A bandpass. The four wavelengths sampled are shown in Table II together with the sensitivities at low and high gain.

Saturation occurs at the 300 kR level for the 5577 Å wavelength, while the noise floor is 2 DN due to electronic origin and the threshold of the intensifier Equivalent Brightness Input at high gain is 15.0 Rayleighs at 5577 Å.

Data storage is effected using a 12-bit A/13 converter. The S/N ratio is optimized by the technique of image summation, in which several images taken in rapid succession are summed in a 512 × 512 × 16-bit video memory. In the normal mode of operation three images, one for each of the auroral wavelengths (4278, 5577, and 6300 Å), are transmitted every 75 s via geostationary satellite to the Ottawa

TABLE II

Sensitivities of the ASI at the various operating wavelengths at high and low gain in digitization numbers (DN) per Rayleigh per second

Wavelength (Å)	Sensitivity high gain (DN Rayleigh^{-1} s^{-1})	Low gain (DN Rayleighs^{-1} s^{-1})
5577	1.400	0.106
4278	0.091	0.017
4400	0.486	0.086
6300	1.310	0.095

TABLE III

System specification for BARS

Transmitter	
Frequency	48.5 MHz
Nominal antenna gain	11 dB
Peak power	50 kW
Pulse length	133 μs
Duty cycle	2
Receiver	
Noise figure	<5 dB
Band width	133 μs matched filter
Nominal antenna gain	22 dB

node. Each image is cropped to a field of view of 140 deg before transmission. An algorithm is provided to produce a compressed image which maps onto the southern part of the area monitored simultaneously by the BARS bistatic auroral radar. These data are available in near real time from the Ottawa node. For high-resolution images, it is necessary to record the raw data on 6250 bpi magnetic tape on site at Gillam. The high-resolution mode can be activated by phoning the unmanned site with instructions for change of mode being done remotely via modem. It is not possible for high resolution data to be recorded at the same time as the BARS mode is functional and *vice versa*.

The ASI functions only when light levels are acceptable. This means recording is restricted to sun down conditions and to conditions when the Moon is either down or the light from the Moon does not exceed 10% of full Moon luminosity.

3.2. BISTATIC AURORAL RADAR SYSTEM (BARS)

The primary purpose of BARS is to provide measurements of the horizontal components of the electric field over an area of the auroral ionosphere shown in Figure 1. The principle of operation of BARS is much the same as that for STARE (Greenwald *et al.*, 1978). Two transmitters located at Nipawin and Red Lake (cf., Table III) send 48.5 MHz signals into the auroral ionosphere using two transmitting and sixteen receiving Yagi antennas at each site. The Yagi receiving antennas, with suitable signal processing, yield sixteen beams with a beam spacing of 3.6 deg, although only the central eight beams are normally used in the data reduction.

Transmission is effected by 50 kW pulses of 133 μs duration radiated by two Yagi antennas. The receiver system consists of 16 identical receiving channels each containing an electronically controlled range variable attenuator and a phase coherent receiver that produces a pair of quadrature outputs, which are required to determine backscatter intensity and Doppler characteristics. Digital processing on-site yields the intensities and Doppler velocities for each of the 50 range cells of each of the pre-selected 8 receiving antenna beams. The modes and operating sequences at the two sites are synchronized to an accuracy of approximately 0.1 s using GOES clocks backed up by crystal oscillators. The data streams from each radar are transmitted via geostationary satellite to the Ottawa node where they are merged into a single data stream and archived. The key parameters for the CDHF are computed in Ottawa.

The normal mode of operation of BARS alternates between single and double pulse transmission. The merging of the individual Doppler velocities from each radar to produce ionospheric vector flow estimates is done using archived data at the time of scientific use of the data. Other radar modes can be implemented independently or interleaved with the normal mode. One of these uses a multiple pulse group of various spacings to determine the autocorrelation function of the backscatter from which the Doppler spectrum can be obtained (cf., Greenwald *et al.*, 1985). Another mode uses high prf coherent pulse-to-pulse transmission, which yields Doppler spectra with higher frequency resolution, similar temporal resolution but lower spatial coverage (cf., Balsley and Ecklund, 1972). In the normal mode, values of the individual radar intensities and the ionospheric flow (viz., electric field) estimates are available every 30 s within a 400 cell array whose grid resolution is 20 km $\times$ 20 km. Further details can be found in the preconstruction paper by McNamara *et al.* (1983).

The aspect angles for the two radars fall in the range of 4–8 deg off perpendicular. Theoretical considerations suggest that there ought not to be echoes at all for such large aspect angles. However, practical experience in the Canadian arctic shows that echoes are, indeed, present during episodes of auroral activity (cf., McNamara, 1972). While there is evidence that refraction of the transmitted signal by regions of high plasma density associated with auroral arcs can reduce some aspect angles to near zero (cf., Hall *et al.*, 1990), this is not always the case, particularly when

extended layers of backscatter are present. Therefore, the threshold values of the merged velocity estimates and their relationship to the actual flow will be treated in the same fashion as they were for the STARE system (Greenwald *et al.*, 1985).

It has been shown that STARE measures well the direction of plasma flow and the variations in both its magnitude and direction but measures the absolute magnitude less well (Nielsen and Schlegel, 1985; Reinleitner and Nielsen, 1985). In fact, the magnitude is progressively undermeasured as its value increases from 500 or 600 m s^{-1}. Similar behaviour is anticipated for BARS. However, a subsequent re-examination of work done using STARE data during the IMS showed that the former three parameters were important in these studies and that the magnitude was of much lesser importance (Nielsen, private communication). In any event, it has been found possible to develop an empirical merge routine for STARE which substantially corrects the magnitude (Nielsen and Schlegel, 1985).

3.3. Magnetometer and Riometer Array (MARIA)

Thirteen of the CANOPUS sites are equipped with a three component magnetometer, zenith riometer and two components of tellurics. For the ISTP/GGS program, only the magnetometer and riometer data will be supplied to the CDHF. The magnetometer array comprises a north-south line through central Canada, and east–west line spanning three time zones from central Canada to close to the Alaska–Yukon border and a shorter north–south line one time zone to the west of Churchill (on the west coast of Hudson Bay as seen in Figure 1).

The magnetometer sensors are of the three axis ringcore type S100 manufactured by Narod Geophysics Limited. They operate over a dynamic range of ±80 000 nT with a sensitivity of $\frac{1}{40}$ nT at an 8 Hz output sample rate. The sensor heads are equipped with tiltmeters that have a resolution of $\frac{1}{128}$ deg as well as a temperature sensor. The temperature response of the detector is of the order of 0.5 nT/°C and the long term stability is in the range of a few nT yr^{-1}.

The riometer is a 30 MHz zenith type manufactured by La Jolla Sciences using a four element antenna and operating with a receiver bandwidth of 250 kHz. This type of riometer provides information on cosmic noise absorption over a region of the ionosphere of radius approximately 100 km centered at the zenith. The level of absorption (in dB) can be quantitatively related to the flux of energetic electrons precipitating into the ionosphere (cf., Bailey, 1968) after subtraction of values provided by a quiet day curve.

Each site is equipped with two-component Earth-current measuring systems, with the electrode pairs being aligned in the geodetic north–south and east–west directions. The system is based on bandpass filter amplifiers covering the frequency range 0.002–2.0 Hz which are connected to copper clad steel electrodes separated by 100 m. The primary task of the tellurics is to characterize the subsurface conductivity structure under each of the magnetometer sites, and the data will not

be supplied on a routine basis to the CDHF although it will be archived in the CANOPUS data base.

All signals (magnetometer, riometer, and tellurics) are sampled at 8 Hz and subsequently the data streams are merged and filtered using a 0.1 Hz lowpass digital filter before yielding one sample every 5 seconds. The samples are then held in a buffer together with housekeeping information on platform status until transmission on successful reception of a GOES clock flag. Data are transmitted by geostationary satellite to the Ottawa node every 2.5 min on average, with each message containing 30 samples of each measured component. In order to permit the acquisition of high resolution data at each site, each platform is equipped with an RS232 port, which permits the data stream to be recorded on suitable user-supplied equipment.

3.4. Meridian scanning photometer array (MPA)

CANOPUS includes four meridian scanning photometers, three of which lie on the meridian through Churchill (viz., Rankin Inlet, Gillam, and Pinawa) with the fourth (Fort Smith) lying about one time zone to the west approximately at the magnetic latitude of Gillam as shown in Figure 1. The instrument at each site is a meridian scanning eight- channel filterwheel photometer. Five of the eight channels measure auroral emissions (6300, 5577, two channels at 4861 and 4709 Å). The three remaining channels (4800, 4935, and 6250 Å) measure background intensities that are used to correct for background emissions.

The instrument scans the meridian twice each minute, with the mirror being stepped through 0.225 deg every time the filterwheel completes a revolution. The filterwheel rotates at 120 rpm, leading to an output of 510 samples per scan per channel. Each sample is corrected for nonlinearity (due to pulse pile-up) and for dark count. Each scan is binned into seventeen latitude bins and the two 4861 Å channels and the two corresponding background channels (4800 and 4935 Å) are averaged. Finally, the resulting scan starting at the even minute and the scan starting 30 s later are averaged. For 4709, 4861, and 5577 Å, bin boundaries are computed assuming an emission altitude of 110 km and the resulting bins are 0.5 deg of latitude in width. For 6300 Å, the emission altitude is assumed to be 250 km and the resulting bins are 1.0 deg of latitude in width. With a field of view of 4° and an entrance pupil of 10 cm, the sensitivity is about 1 count Rayleigh^{-1} for each averaged measurement. Dark count is measured once per hour on the half hour and a calibration is performed once per hour on the hour using an internal calibration source. The instruments operate fully automatically during periods when the solar Zenith angle is $> 96°$, and they utilize a built-in solar ephemeris routine and a two-level dawn-dusk sensor for controlling the operating periods.

Every two minutes, each instrument transmits two scans in the four auroral emissions and two background channels as well as the housekeeping data. The housekeeping data include the instrument dark count, the auto-calibration data

and the other instrument status information such as photomultiplier tube and filter temperatures, and light sensor and calibration voltages. As in the case of the MARIA instrumentation, there is a campaign port at each site (RS-232, 4800 baud) which permits a parallel readout of all 510 samples for each channel. Thus, it is possible to obtain data at a rate of one scan every 30 s on site, as compared to the nominal one scan per minute available via satellite link.

3.5. Data collection system (DCS)

The transmission from the sites to the central receiving node in Ottawa is via an Anik geostationary communications satellite at frequencies of 14 GHz for the uplink and 12 GHz for the downlink. The transmission is one way according to a schedule stored at each of the sites. The data are stored in a buffer and are transmitted in block sizes of approximately 500 bytes every 2–3 minutes for the MARIA and MPA instruments and approximately every 30 s for the BARS. The data are accepted in Ottawa, are passed through PC-based synchronous- to-asynchronous converters and are ported to a MicroVAX 3900 cluster and a MicroVAX 3100 hot standby. The ASI data are transmitted continuously at an average baudrate of 12.5 kB using digital modems with full error correction protocol. The data are ported directly to two MicroVAX processors. The data can be accessed in near real time through accounts on the Ottawa node CANOTT. Once a day, the raw (alpha) data are processed and they remain on-line for 14 days with the processed beta data staying on line for one month. After 14 days, data are archived on 8 mm tape. Once a month, data are distributed to all CANOPUS teams so that the scientific studies can be carried out at the home institutions of the various investigators. The total volume of alpha data received ranges from 100 Mbytes day^{-1} in midwinter at lunar darkness to 20 Mbytes day^{-1} in midsummer and at full Moon. Key parameters are constructed from these data every day for the preceding day and are supplied to the CDHF daily. The Key Parameters and their descriptions are found in Appendix A.

4. Sample Data From the CANOPUS Network

In this final section, we shall present data from one sample event, illustrating the standard formats in which information of the various instruments is presented at the first stage of data processing. We have selected a typical interval of substorm activity, recorded on November 14, 1993 in the UT interval 04:00–08:00.

Figure 2 presents the magnetometer data from the Churchill line part of the array in the form of stack plots. Only the geographic north–south (X) component is shown here, although the east–west (Y), and vertical (Z) components can be plotted in a similar format. The dotted horizontal lines reflect the mean of the data over the time covered by the plot, and the absolute value of the field reflected by that mean and the station identification is plotted on the left side of the figure.

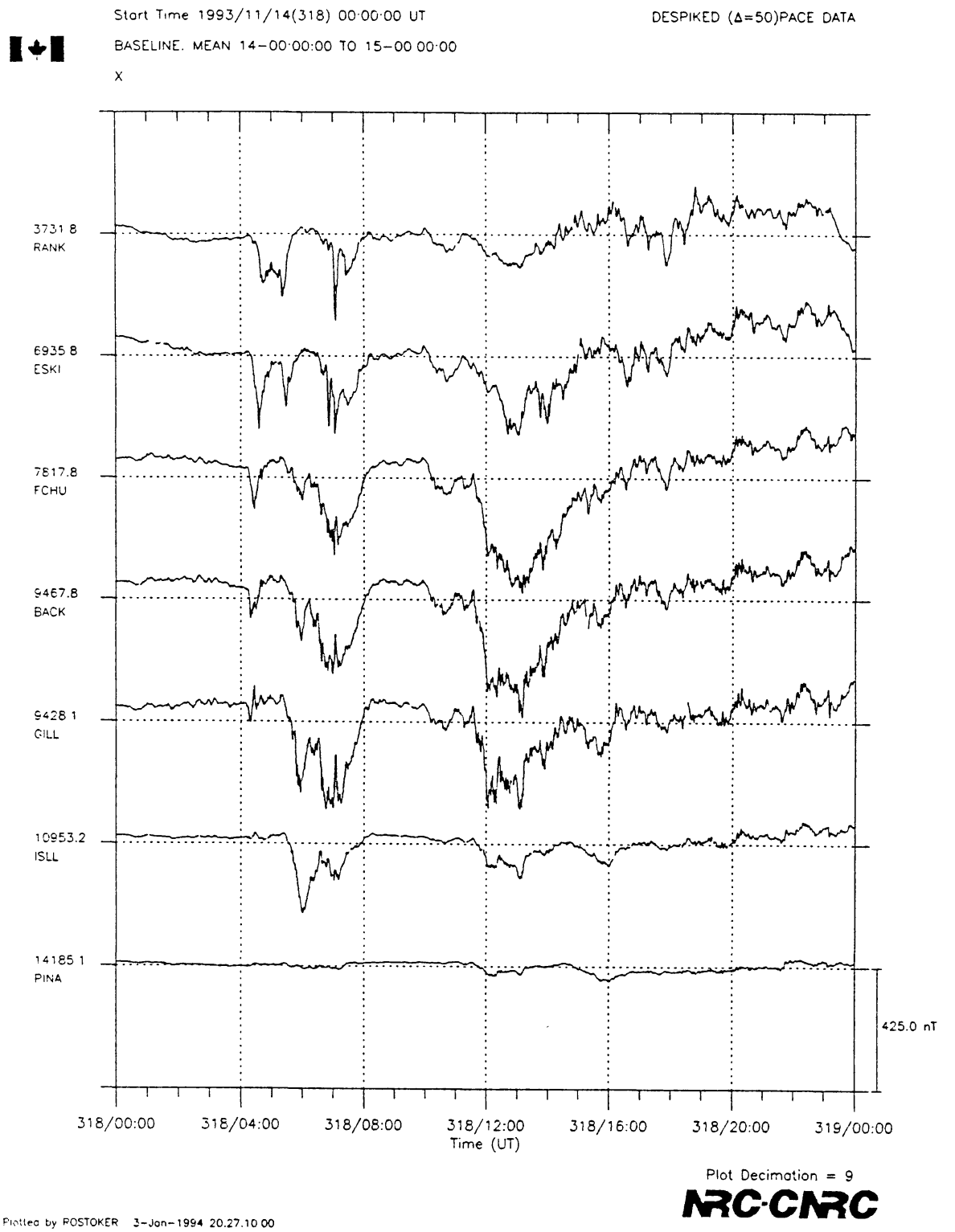

Fig. 2. X-component magnetograms from the the Churchill line portion of the CANOPUS magnetometer array. These data cover the UT day November 14, 1993 (Day 318). The station acronyms used in the CANOPUS program are shown along the ordinate axis beside the record for each station along with the value of the total X-component field at those stations averaged over the 24 hours of data plotted. For demonstration purposes in this paper, the data in the interval 04:00–08:00 UT will be examined more closely with the aid of data obtained from the other instrumentation at the CANOPUS stations.

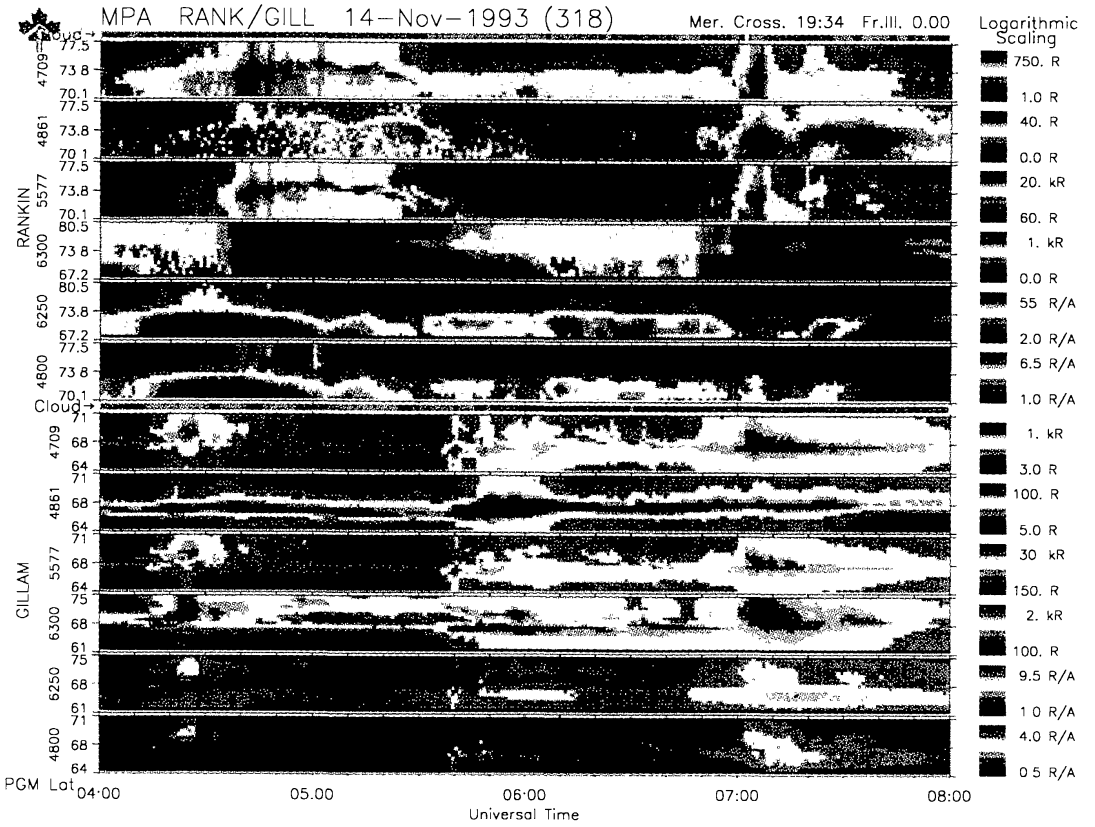

Fig. 3. (*Top of Plate 1*). Meridian scanning photometer data from the Gillam and Rankin Inlet for the interval 04:00–08:00 UT on November 14, 1993. All four auroral wavelengths together with the two wavelengths used to subtract background contamination are shown for both stations. Coloured bars at the top of each panel give an indication of the presence or lack of cloud contamination. Three substorm expansive phase onsets are visible within this time period (see text).

The UT and Day of Year (January 1 = Day 1) appear on the abscissa and the start time of the plot is indicated at the top of the figure. The seven stations from the top of the figure range from the highest latitude station, Rankin Inlet (RANK) to the lowest latitude station, Pinawa (PINA) (see Table I). This event features the initiation of expansive phase activity at $\sim$ 04 : 15 UT at high latitudes (ESKI), with ensuing expansive phase intensifications appearing at lower latitudes around $\sim$ 05 : 40 UT (ISLL) and $\sim$ 06 : 45 UT (GILL).

Figure 3 shows the meridian scanning photometer (MPA) data from the average auroral zone station of Gillam and the high latitude station of Rankin Inlet on the Churchill line. All six wavelengths for each station are shown in this plot format, the latitudes along the ordinate axis being in PACE invariant coordinates. The colour bar scales on the left side of the plot indicate the intensity of the luminosity in units of rayleighs (R) or kilorayleighs (kR) for the main auroral wavelengths and R/Å for the two background channels of 4800 and 6250 Å. This night features some cloudy intervals, as indicated by the horizontal bar at the top of the plot (green indicating clear sky conditions and red indicating the presence of clouds). Intense signals at one latitude are spread vertically by the presence of clouds, an example being apparent at 05:40 UT at Gillam. The onsets identified by the magnetometers are clearly visible in the photometer record, particularly those at

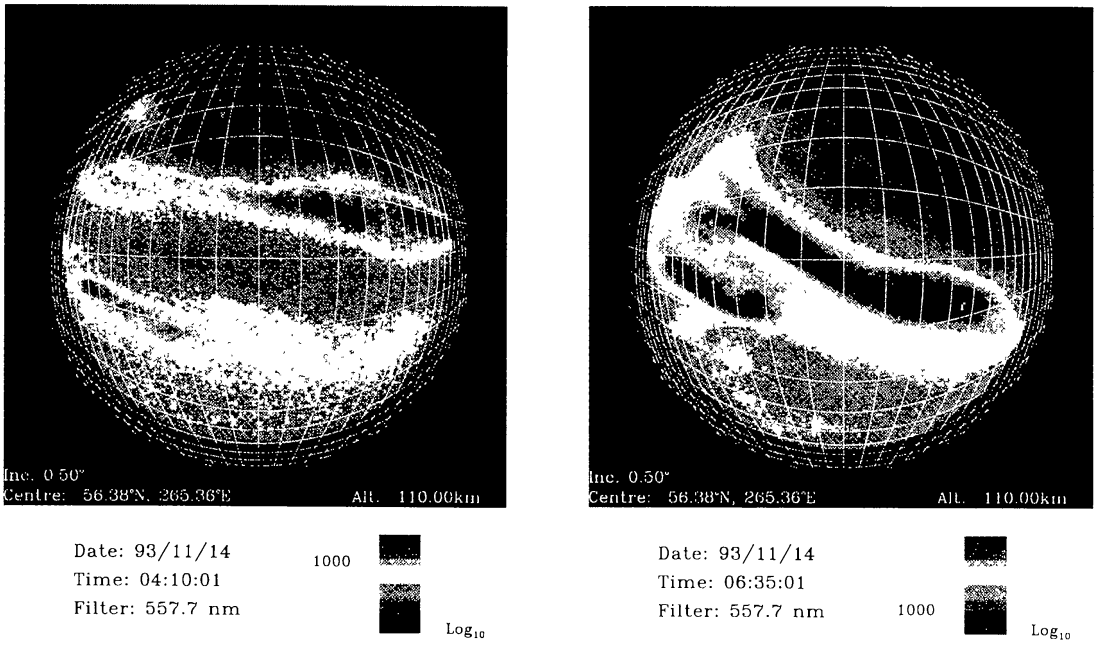

Fig. 4. (*Bottom of Plate 1*). ASI images taken at the 5577 Å wavelength at two instants (04:10:01 UT and 0635:01 UT) on November 14, 1993 with exposure times of 1.7 s. The grid shown on the image is in geographic coordinates with adjacent lines being separated by 0.5 deg and the center of the image being at geographic coordinates shown at the left corner of the image.

~04:15 and ~05:40 UT. Two latitudinally separated regions of luminosity are visible after the 04:15 UT expansive phase onset, with both regions of the oval intensifying around the time of the 05:40 UT onset. At Gillam, the higher latitude region is clearly more intense than the lower latitude region prior to local midnight (~06:00 UT) and this situation is reversed after local midnight. The 06:45 UT onset is less clear in the photometer record, however a subsequent intensification just prior to ~07:00 UT involves an explosive poleward expansion which is best seen in the Rankin Inlet record and which is also evident in the magnetometer data shown in Figure 2.

Figure 4 shows two ASI images taken at the 5577 Å wavelength at two instants (04:10:01 and 06:35:01 UT) during the period of activity covered by the magnetometer and photometer data shown above. A grid of geographic coordinate lines is superposed on each image, the center of the grid corresponding to 56.38 °N, 265.36°E geographic and the separation between adjacent grid lines being 0.5°. The image at 0410:01 features two parallel arcs separated by 100 km with this double arc feature also being visible in the MPA data from Gillam shown in Figure 3. The multiple arc structure in the image taken at 06:35:01 UT is more blurred because of the strong diffuse auroral background, however the signature of the brighter arc near the zenith at Gillam is visible in the MPA data as well. The MPA and ASI data complement one another in providing a two-dimensional view of the aurora on one hand (courtesy the ASI) and multiple wavelength coverage across the two dimensional image (courtesy the MPA).

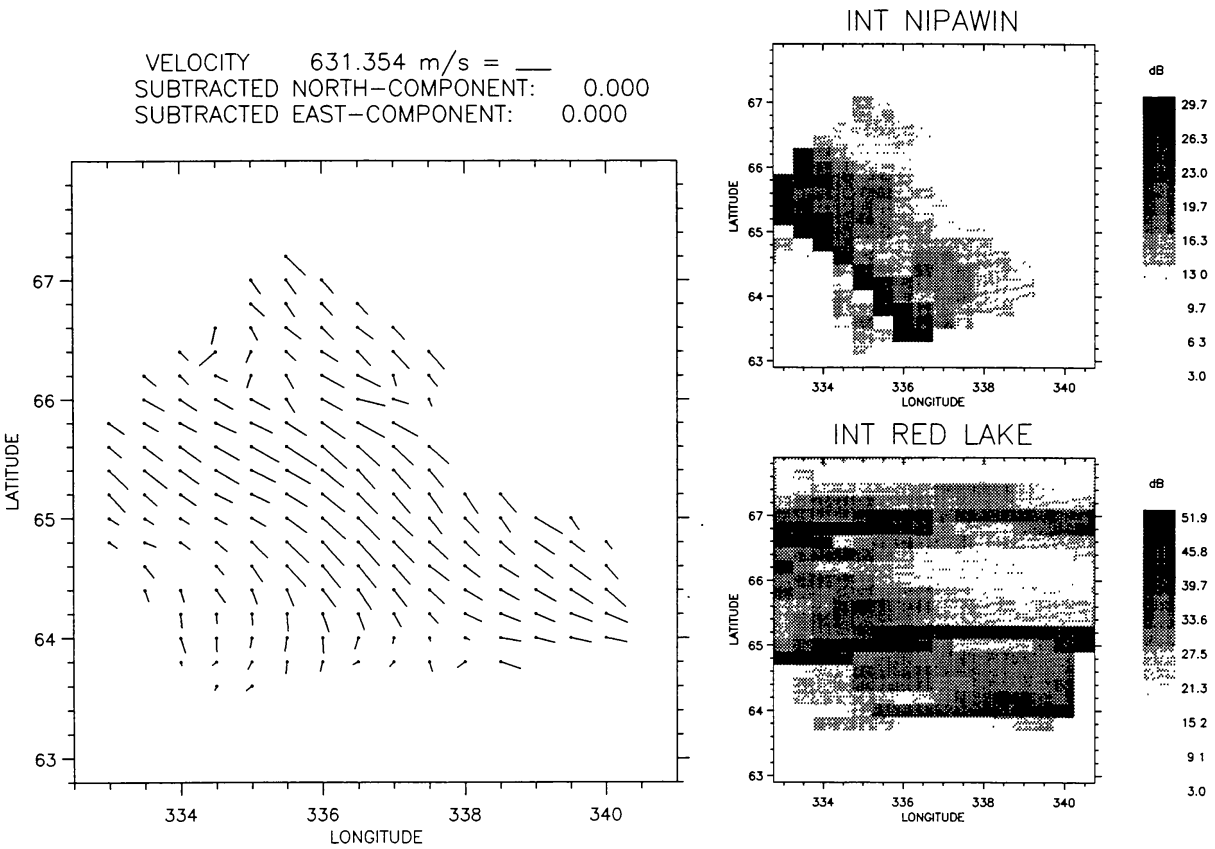

Fig. 5. BARS data for 06:35:30 UT on November 14, 1993 showing the drift velocities (assumed to reflect $\mathbf{E} \times \mathbf{B}$ drift) and intensity of the echoes received at the two receiver sites whose coordinates are given in Table I. The coordinates on this figure are eccentric dipole field line (EDFL) coordinates, with 337° EDFL longitude corresponding to ~ 330° in PACE invariant coordinates and 64° EDFL latitude corresponding to ~ 67° in PACE invariant coordinates.

Figure 5 shows one of the representations of the BARS auroral radar data, emphasizing the ionospheric drift vectors in the field of view of the ASI (from which the ionospheric electric field configuration can be inferred). In addition, the strength of the scattered radar signals received by the two radars at Nipawin and Red Lake is presented in the panels on the right hand side of the figure. This gives a picture the the locale of the discrete auroral features in the field of view of the radar. This particular data set pertains to the 06:35:01 UT image shown on the right side of Figure 4.

5. Conclusion

The CANOPUS array is a state-of-the-art complement of instruments which is able to characterize the ionosphere over north–central and north–western Canada to the extent of allowing ISTP/GGS researchers flying payloads aboard the mission satellites to better interpret their data. The CANOPUS data can be inspected initially using the key parameters supplied to the CDHF within 24 hours of their

acquisition, although these data are not suitable for scientific studies. The data to be used for scientific studies reside on 8 mm exabyte tape at each of the nodes of the CANOPUS network. Data may be accessed in near real time through arrangements which may be made by contacting the Principal Investigator, G. Rostoker. Studies may be initiated by making contact with an appropriate CANOPUS Team member, and requests for data can be made through the Principal Investigator (at E-mail addresses rostoker@space.ualberta.ca or canedm::rostoker). All joint studies are carried out under the CANOPUS 'Rules of the Road' which are supplied to collaborators with CANOPUS Team members at the start of the collaboration.

Acknowledgements

CANOPUS is financed by the Canadian Space Agency. As it has evolved, CANOPUS has benefitted greatly from the generous deployment of the resources of the National Research Council of Canada by the present and past Directors of the Herzberg Institute of Astrophysics. Research activity utilizing CANOPUS data is supported, in part, by the Natural Sciences and Engineering Research Council of Canada.

1995SSRv...71..743R

Appendix A

CANOPUS key parameters

CANOPUS component	Frequency	Key parameter	Description
BARS	Every minute	Drift velocity	North–south and east–west component of plasma drift for 15 cells along the 226.5° EDFL meridian from 64.2°–67.0° EDFL
		Numbers of vectors	Number of maps points with measurable velocites (out of 400)
MARIA	Every minute	CU and CL index	Value of the extrema of sign$(x)\sqrt{(x^2+z^2)}$ over the array
		Latitude, longitude	Coordinates of the sites where the extreme occurred
		Site availability	Operational status of each site
		Average riometer absorption	Average of the absorption along the Churchill line
		Peak riometer absorption	Peak absorption along the Churchill line
		Latitude, longitude	Coordinates of the site where the extreme occurred
		Site availability	Operational status of each site
MPA	Every minute	Merged scans	Scaled merged 5577 Å scans along the Chuchill line
		Peak intensity	Intensity of the brightest cell of the merged scan
		Station status	Operational status and cloud index of all MPA sites
ASI	Every 5 min	Image	Scaled image in 5577 Å, mapped to the BARS observing area
		Peak intensity	Intensity of the brightest cell of the image

References

Akasofu, S.-I., Stenbaek-Nielsen, H. C., Hallinan, T. J., Rostoker, G., and Baker, D. N.: 1992, *EOS* **73**, 305.

Bailey, D. K.: 1968, *Rev. Geophys.* **6**, 1968.

Baker, K. B. and Wing, S.: 1989, *J. Geophys. Res.* **94**, 9139.

Balsley, B. B. and Ecklund, W. L.: 1972, *J. Geophys. Res.* **77**, 4746.

Birkeland, K.: 1908, *The Norwegian Aurora Polaris Expedition 1902–1903* **1**, 1st Section.

Carpenter, D. L.: 1963, *J. Geophys. Res.* **68**, 1675.

Feldstein, Ya. I., Levitin, A. E., Faermark, D. S., Afonina, R. G., and Belov, B. A.: 1984, *Planetary Space Sci.* **39**, 907.

Greenwald, R. A., Weiss, W., Nielsen, E., and Thomson, N. R.: 1978, *Radio Sci.* **13**, 1021.

Greenwald, R. A., Baker, K. B., Hutchins, R. A., and Hanuise, C.: 1985, *Radio Sci.* **20**, 63.

Hall, G., Moorcroft, D. R., Cogger, L. L., and Andre, D.: 1990, *J. Geophgs. Res. 95*, 15281.

Jelly, D. H. and Brice, N.: 1967, *J. Geophys. Res.* **72**, 5919.

Kamide, Y., Richmond, A. D., and Matsushita, S.: 1974, *J. Geophys. Res.* **86**, 801.

Kisabeth, J. L. and Rostoker, G.: 1974, *J. Geophys. Res.* **79**, 972.

McNamara, A. G.: 1972, *Geofys. Publik.* **29**, 135.

McNamara, A.G., McDiarmid, D. R., Sofko, G. J., Koehler, J. A., Forsyth, P. A., and Moorcroft, D. R.: 1983, *Adv. Space Res.* **2**, 145.

Mishin, V. M., Bazarzhapov, A. D., and Shpynev, G. B.: 1980, in S.-I. Akasofu (ed.), *Dynamics of the Magnetosphere*, D. Reidel Publ. Co., Dordrecht, Holland, p. 249.

Nielsen, E. and Schlegel, K.: 1985, *J. Geophys. Res.* **90**, 3498.

Rees, M. H.: 1989, *Physics and Chemistry of the Upper Atmosphere*, Cambridge University Press, Cambridge.

Reinleitner, L. A. and Nielsen, E.: 1985, *J. Geophys. Res.* **90**, 8477.

Richmond, A. D. and Kamide, Y.: 1988, *J. Geophys. Res.* **93**, 5741.

Rostoker, G.: 1990, in B. Hultqvist and C.-G. Fälthammar (eds.), *Magnetospheric Physics*, Plenum Press, New York, p. 115.

Vestine, E. H. and Chapman, S.: 1938, *Terrest. Magnetism Atmospheric Elec.* **43**, 351.

Wiens, R. G. and Rostoker, G.: 1975, *J. Geophys. Res.* **80**, 2109.